

Precision Measurements of Charmonium States Formed in $\bar{p}p$ Annihilation

T. A. Armstrong,⁽⁶⁾ D. Bettoni,⁽²⁾ V. Bharadwaj,⁽¹⁾ C. Biino,⁽⁷⁾ G. Borreani,⁽²⁾ D. Broemmelsiek,⁽⁴⁾ A. Buzzo,⁽³⁾ R. Calabrese,⁽²⁾ A. Ceccucci,⁽⁷⁾ R. Cester,⁽⁷⁾ M. D. Church,⁽¹⁾ P. Dalpiaz,⁽²⁾ P. F. Dalpiaz,⁽²⁾ J. E. Fast,⁽⁴⁾ S. Ferroni,⁽³⁾ C. M. Ginsburg,⁽⁵⁾ K. E. Gollwitzer,⁽⁴⁾ A. A. Hahn,⁽¹⁾ M. A. Hasan,⁽⁶⁾ S. Y. Hsueh,⁽¹⁾ R. A. Lewis,⁽⁶⁾ E. Luppi,⁽²⁾ M. Macrì,⁽³⁾ A. Majewska,⁽⁶⁾ M. A. Mandelkern,⁽⁴⁾ F. Marchetto,⁽⁷⁾ M. Marinelli,⁽³⁾ J. L. Marques,⁽⁴⁾ W. Marsh,⁽¹⁾ M. Martini,⁽²⁾ M. Masuzawa,⁽⁵⁾ E. Menichetti,⁽⁷⁾ A. Migliori,⁽⁷⁾ R. Mussa,⁽⁷⁾ S. Palestini,⁽⁷⁾ N. Pastrone,⁽⁷⁾ C. Patrignani,⁽³⁾ J. Peoples, Jr.,⁽¹⁾ L. Pesando,⁽⁷⁾ F. Petrucci,⁽²⁾ M. G. Pia,⁽³⁾ S. Pordes,⁽¹⁾ P. A. Rapidis,⁽¹⁾ R. E. Ray,^{(1),(5)} J. D. Reid,⁽⁶⁾ G. Rinaudo,⁽⁷⁾ J. L. Rosen,⁽⁵⁾ A. Santroni,⁽³⁾ M. Sarmiento,⁽⁵⁾ M. Savrié,⁽²⁾ J. Schultz,⁽⁴⁾ K. K. Seth,⁽⁵⁾ G. A. Smith,⁽⁶⁾ L. Tecchio,⁽⁷⁾ F. Tommasini,⁽³⁾ S. Trokenheim,⁽⁵⁾ M. F. Weber,⁽⁴⁾ S. J. Werkema,⁽¹⁾ J. L. Zhao,⁽⁵⁾ and M. Zito⁽³⁾

(E-760 Collaboration)

⁽¹⁾Fermi National Accelerator Laboratory, Batavia, Illinois 60510

⁽²⁾Istituto Nazionale di Fisica Nucleare and University of Ferrara, 44100 Ferrara, Italy

⁽³⁾Istituto Nazionale di Fisica Nucleare and University of Genoa, 16146 Genoa, Italy

⁽⁴⁾University of California at Irvine, Irvine, California 92717

⁽⁵⁾Northwestern University, Evanston, Illinois 60201

⁽⁶⁾Pennsylvania State University, University Park, Pennsylvania 16802

⁽⁷⁾Istituto Nazionale di Fisica Nucleare and University of Turin, 10125 Turin, Italy

(Received 13 November 1991; revised manuscript received 3 February 1992)

Fermilab experiment E-760 studies the resonant formation of charmonium states in proton-antiproton interactions using a hydrogen gas-jet target in the Antiproton Accumulator ring at Fermilab. Precision measurements of the mass and width of the charmonium states χ_{c1}, χ_{c2} , a direct measurement of the ψ' width, and a new precision measurement of the J/ψ mass are presented.

PACS numbers: 14.40.Gx, 13.75.Cs

We report the first results from Fermilab experiment E-760, a study of charmonium states formed directly in proton-antiproton annihilation. We present the first measurement of the total width of the χ_{c1} (3P_1), and improved measurements of the χ_{c2} (3P_2) total width and of the masses of both resonances. We also report the first direct measurement of the total width of the ψ' and a new measurement of the mass of the J/ψ .

The experiment uses a beam of antiprotons circulating in the Fermilab Antiproton Accumulator ring [1] and an internal hydrogen gas-jet target to study charmonium states formed in the exclusive reaction $\bar{p}+p \rightarrow (\bar{c}c)$, a technique first exploited at the CERN Intersecting Storage Rings [2]. States of all allowed J^{PC} are formed directly in $\bar{p}p$ annihilation while only states of $J^{PC}=1^{--}$ are made directly in e^+e^- annihilation. In $\bar{p}p$ annihilations, however, the $(\bar{c}c)$ formation cross sections are as small as 1 part in 10^6 of the total cross section and it is not feasible to detect these states through their hadronic decays. Nevertheless, by selecting the decay modes $\bar{c}c \rightarrow J/\psi + X$, $J/\psi \rightarrow e^+e^-$, an almost background-free sample can be obtained.

The masses and widths of the $(\bar{c}c)$ states are determined directly from the antiproton beam energy by measuring the excitation curves of the resonances as the energy of the antiproton beam is changed in small steps. The resonances were scanned by decelerating the antipro-

ton beam from the accumulation energy of 8.9 GeV to an energy just above the resonance and then decelerating in steps of between 170 and 500 keV (center-of-mass energy) depending on the resonance. In the present experiment, the antiproton beam was cooled to $(\Delta p/p)_{\text{rms}} \approx 2 \times 10^{-4}$. This produced a spread in the center-of-mass energy, ΔW , of 240 keV, thus allowing a direct measurement of sub-MeV widths for the charmonium states.

The results presented here depend on our knowledge of two parameters of the antiproton beam: the absolute value of the beam momentum and the beam momentum spread. The beam momentum is most precisely derived from the beam velocity measured from the revolution frequency f_r and the orbit length L_o . Since the revolution frequency is measured with a precision of approximately 2 parts in 10^7 , the major uncertainty in determining the velocity of the beam comes from the knowledge of the orbit length. Conventional surveying techniques proved not sufficiently precise and so a reference orbit length L_{ref} was determined by performing an energy scan at the ψ' and taking the value of the ψ' mass from the literature. The 0.1-MeV/ c^2 uncertainty in this mass [3] produces a 0.7-mm systematic uncertainty in L_{ref} .

Repeated scans at the J/ψ showed a reproducibility of the center-of-mass energy setting to better than 0.05 MeV/ c^2 which corresponds to a further uncertainty of 1 mm in the total orbit length of 474.046 m. This is con-

sistent with the intrinsic resolution of the beam position monitors which are used to correct for small changes between the reference orbit and the orbits actually used in the scans of the resonances.

To determine the true resonance widths, the beam momentum distribution must be unfolded from the observed excitation curves. This distribution is derived from the beam-revolution-frequency spectrum using the relation $\Delta p/p = (1/\eta)\Delta f_r/f_r$, where η depends on the setting of the Accumulator lattice. The beam-revolution-frequency spectrum itself is obtained with high precision by Fourier analysis of the beam current Schottky noise. This spectrum, which is recorded every three minutes during data taking, is well parametrized by a slightly asymmetric Gaussian shape [4].

For the χ_{c1} and the χ_{c2} , the resonance width is significantly larger than ΔW and the value of η is obtained with sufficient precision from the measured synchrotron oscillation frequency. Our experiment also yields a direct measurement of the ψ' width even though the energy spread of the beam is larger than the width of the resonance. This result can be understood if one considers, as an example, the properties of the convolution of a Breit-Wigner form with a Gaussian distribution. In such a case, the observed peak cross section for $\Gamma_{\text{beam}} > \Gamma_{\text{res}}$ is approximately

$$\sigma_{\text{peak}} \approx \sqrt{4 \ln 2 / \pi} (A / \Gamma_{\text{beam}}) (1 - \sqrt{4 \ln 2 / \pi} \Gamma_{\text{res}} / \Gamma_{\text{beam}}),$$

where A is the integral of the resonance cross section. The last term in parentheses shows that the resonance width has a linear effect on the observed peak cross section. For $\Gamma_{\text{res}}/\Gamma_{\text{beam}} \ll 1$, this term is 1 and the observed peak cross section depends only on the beam energy spread. In our case, however, this term, had we approximated our beam as a Gaussian, would be 0.6 at the ψ' and a direct measurement of $\Gamma_{\psi'}$ can be obtained from the shape of the excitation curve. Here a precise knowledge of η is essential, and a novel "double-scan" technique [5] was developed to give a second and independent measurement of its value. In this technique, the deceleration for each energy step through the scan was performed in two stages. The first stage involved measuring the resonance cross section with the beam at a known energy, E_c^i , on the central orbit of the Accumulator. The beam was then decelerated one step without changing the Accumulator magnetic field. The deceleration reduced the beam energy by an amount ΔE , changed the revolution frequency by an amount Δf_r^i , and moved the beam onto a "side" orbit where the cross section at this new energy, E_s^i , was again measured. The Accumulator magnetic field was then reduced to return the beam to the central orbit, the cross section was measured, and the process repeated throughout the resonance scan. The data thus obtained consist of a set of cross-section measurements at known energies E_c^i and a second set measured at energies E_s^i , where $E_s^i = E_c^i + (1/\eta)\gamma m_p \beta^2 \Delta f_r^i/f_r^i$. The value of η is found, in essence, by forcing the excitation curve from the

side-orbit data to match the central-orbit curve. The value of η thus obtained agrees well with the value from the synchrotron frequency measurement.

Figure 1 shows a cut through the E-760 apparatus [6]. The intersection of the gas jet and the antiproton beam produces an interaction region about 0.5 cm on a side. The detector has a large acceptance and is optimized for the identification of electromagnetic final states from charmonium decay. It covers the complete azimuth (ϕ) and from 2° to 70° in polar angle (θ). The central and forward calorimeters identify electrons and photons and measure their energies and directions. The central calorimeter covers the region $12^\circ < \theta < 70^\circ$. The apparatus inside it consists, from the beam pipe out, of an inner scintillation-counter hodoscope, two layers of longitudinal straw tubes which provide information in both ϕ and θ , a radial projection chamber (RPC) and a multiwire proportional chamber (MWPC) with cathode readout to provide θ information, a second scintillation-counter hodoscope, and a multicell threshold Cherenkov counter for electron identification. The outermost tracking devices in the central region are two layers of Iarocci tubes with cathode readout for θ and ϕ information ($68^\circ > \theta > 22^\circ$), and a planar MWPC ($18^\circ > \theta > 10^\circ$). The central electromagnetic calorimeter itself consists of a cylindrical array of 1280 lead-glass Cherenkov counters each pointing to the interaction region. The forward region ($2^\circ < \theta < 12^\circ$) is instrumented with an eight-element hodoscope, and a 144-channel Pb/scintillator calorimeter preceded by three planes of straw tubes. An array of silicon detectors covering the polar angle region from 82° to 90° measures the yield of elastic-recoil protons and provides the luminosity monitor.

The experimental trigger for these data was designed to select all ($c\bar{c}$) decays to a final state with a J/ψ decaying to e^+e^- in the acceptance of the central calorimeter. This was implemented by requiring two electron "tracks" as defined by the hodoscopes and the appropriate cells in the Cherenkov counters and two high-energy clusters in the central electromagnetic calorimeter.

The invariant mass of the candidate electron-positron pair, m_{ee} , was calculated from measured cluster energies

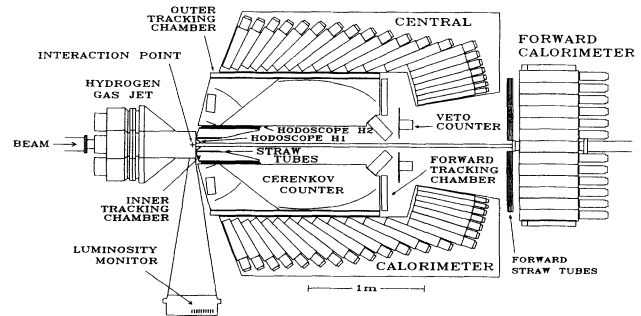


FIG. 1. A cut through the E-760 detector.

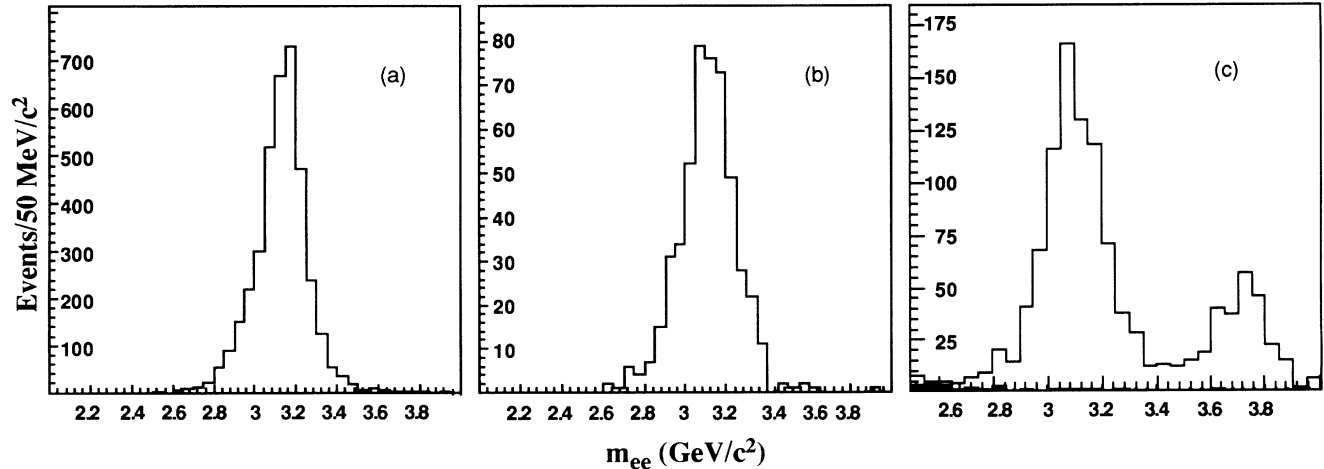


FIG. 2. The reconstructed invariant mass of candidate electron pairs for events at (a) the J/ψ formation energy, (b) the χ_{c2} formation energy, and (c) the ψ' formation energy (open area) and just off resonance normalized to the same luminosity (solid area).

and track angles. The event selection was based on the final-state topology and electron "quality" depending on the resonance. For events found at the J/ψ formation energy the simple requirement of exactly two clusters in the central calorimeter was sufficient to obtain a clean J/ψ sample as is evident from the reconstructed mass distribution of Fig. 2(a). For the χ_c states remarkably clean signals are found in the channel $\chi_c \rightarrow J/\psi + \gamma$, $J/\psi \rightarrow e^+e^-$ by performing a kinematic fit to the three-body final state. Figure 2(b) shows the m_{ee} distribution for events which satisfy the kinematic fit in the χ_{c2} energy scan. Finally, the ψ' sample relied only on the identification of two good electron candidates obtained by cuts on the amplitudes of the signals from the hodoscopes, the RPC, and the Cherenkov counters, and on the shape of the calorimeter energy deposition. In each case the background level was obtained empirically from data taken off resonance by applying the same event selection criteria. Figure 2(c) shows the m_{ee} distribution for events found at the ψ' formation energy. The two peaks correspond to the inclusive decay $\psi' \rightarrow J/\psi + X$, $J/\psi \rightarrow e^+e^-$ and the exclusive decay $\psi' \rightarrow e^+e^-$. The background event distribution, normalized to the on-resonance luminosity, is just visible as the solid area on Fig. 2(c). Table I lists the luminosity taken at each resonance, the total number of events found, and the estimated number of background events under the resonance.

TABLE I. Data for each resonance scan.

Resonance	P_{beam} (MeV/c)	Luminosity (nb) ⁻¹	Total no. of events	Estimated background
J/ψ	4066	360	~4000	8 ± 3
χ_{c1}	5550	1030	503	19 ± 3
χ_{c2}	5724	1160	569	22 ± 4
ψ'	6232	1493	1624	27 ± 4

The results presented here depend only on the stability of the apparatus over the period of a scan, and *do not depend* on a determination of an absolute cross section. The luminosity monitor was stable to better than 1.5% (rms), as evidenced by cross-checks with rates in the scintillation-counter hodoscopes. The trigger and reconstruction efficiency was stable to better than 1%. The overall event acceptance and efficiency was approximately 40%. Variations in the apparatus' response due to the change in energy over a scan were negligible.

The masses and widths of the χ_{c1} and χ_{c2} states are calculated by a maximum-likelihood fit of the number of events per unit luminosity found at each point of the energy scan, by a Breit-Wigner form convoluted with the measured beam energy distribution plus a constant background. For the ψ' , the fit uses the data from both the central and the side orbits simultaneously to yield η directly as well as the resonance width. Figure 3 shows the excitation cross sections measured with energy scans at the χ_{c1} , χ_{c2} , and ψ' . The solid lines are the convolution of the Breit-Wigner resonance form with the beam energy distribution; the dashed lines show a typical resolution in the center-of-mass energy.

The results of the fits are given in Table II. For the mass measurements, the first error given is statistical; the second is the systematic error which arises from the uncertainty in the mass of the ψ' and the 1-mm resolution in the measurement of the orbit length. Since the two χ_c masses are so close, the mass difference, $M_{\chi_{c2}} - M_{\chi_{c1}}$, is hardly affected by the uncertainty in the ψ' mass. For the width measurements, the first error given is again statistical and the second systematic. For the χ_c states, the systematic error is due to the uncertainty in determining η and thus the beam momentum spread. For the ψ' , the effect of the uncertainty in η is included in the statistical error of the fit to the double-scan data; the systematic uncertainty arises from the treatment of the beam frequency spectrum and from variations in the central-orbit

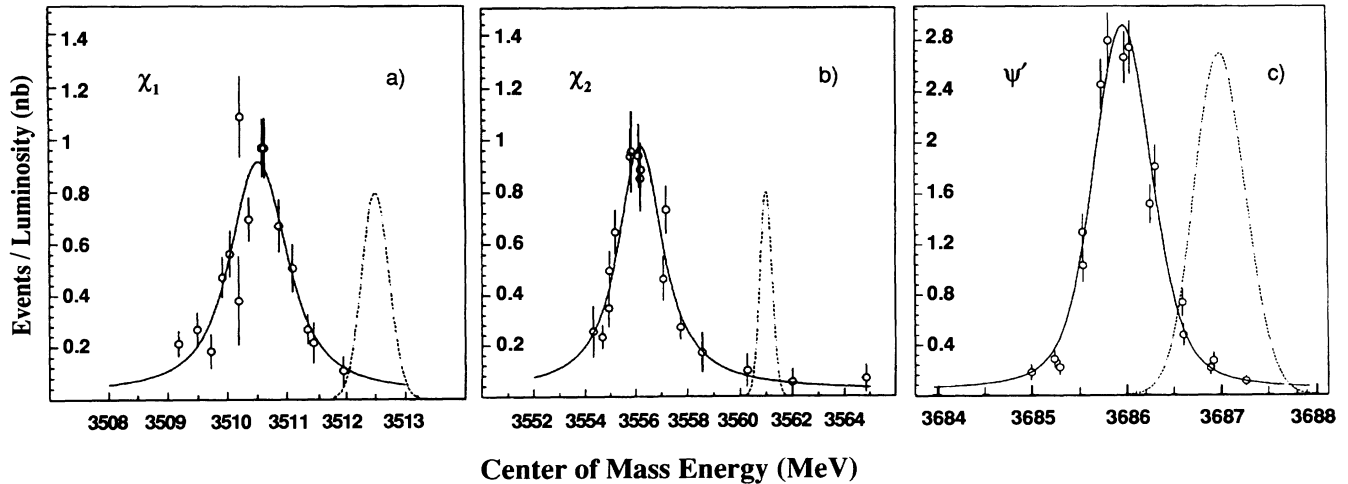


FIG. 3. Events per unit luminosity for the energy scan at (a) the χ_{c1} , (b) the χ_{c2} , and (c) the ψ' . The solid line represents the best fit with the data. The dashed line shows a typical resolution in the center-of-mass energy (arbitrary vertical units).

length. The effects of radiation in the initial state on the observed masses and widths are much smaller than the errors quoted and no corrections have been applied.

The uncertainty in the reference-orbit length contributes only $33 \text{ keV}/c^2$ to the systematic error in the mass of the J/ψ and results in a measurement with slightly better accuracy than previously reported [3]. For the masses of the χ_{c2} and χ_{c1} the new values agree well with previous ones and the errors are reduced by a factor of more than 2. The width of the χ_{c1} has been measured for the first time and the uncertainty on the χ_{c2} width has been reduced from $\sim 40\%$ to $\sim 10\%$. The measurements of these total widths can be used to obtain the partial widths for radiative and hadronic decays. A comparison of these partial widths with theoretical predictions will be presented elsewhere [6]. Our value for the ψ' width, derived from the shape analysis of the excitation curve, is somewhat higher than the value obtained at e^+e^- machines which is derived from integrated cross-section measurements.

TABLE II. Resonance parameters.

Resonance	Mass (MeV/c^2)	Width (keV)
J/ψ (this expt.)	$3096.88 \pm 0.01 \pm 0.06$	
J/ψ (Ref. [7])	3096.93 ± 0.09	68 ± 10
χ_{c1} (this expt.)	$3510.53 \pm 0.04 \pm 0.12$	$880 \pm 110 \pm 80$
χ_{c1} (Ref. [7])	3510.6 ± 0.5	< 1300
χ_{c2} (this expt.)	$3556.15 \pm 0.07 \pm 0.12$	$1980 \pm 170 \pm 70$
χ_{c2} (Ref. [7])	3556.3 ± 0.4	2600^{+1200}_{-900}
ψ' (this expt.)	3686.0 (input)	$308 \pm 36 \pm 16$
ψ' (Ref. [7])	3686.0 ± 0.1	243 ± 43
$\chi_{c2} - \chi_{c1}$ (this expt.)	$45.62 \pm 0.08 \pm 0.12$	

We gratefully acknowledge the technical support from our collaborating institutions and the outstanding contribution of the Fermilab Accelerator Division Antiproton Department. This work was funded by the U.S. Department of Energy, the National Science Foundation, and by the Italian Istituto Nazionale di Fisica Nucleare.

- [1] J. Peoples, Jr., in *Low Energy Antimatter, Workshop on the Design of a Low Energy Antimatter Facility, October 1985*, edited by D. Cline (World Scientific, Singapore, 1986), p. 144.
- [2] C. Baglin *et al.*, Nucl. Phys. **B286**, 592 (1987).
- [3] A. A. Zholentz *et al.*, Phys. Lett. **96B**, 214 (1980).
- [4] A Gaussian with different widths for the high- and low-energy sides (typically $\sigma_{\text{low}}/\sigma_{\text{high}} \approx 1.12$) fits the data well down to the 0.1% level where we observe a low-energy tail due to energy straggling in the target. We have used a more elaborate parametrization that includes higher-order terms and a contribution from the low-energy tail to fit each spectrum. Uncertainties due to the form of the parametrization and averaging procedure have been included in the quoted systematic errors.
- [5] S. Y. Hsueh *et al.*, in Proceedings of the International Conference on Hadron Spectroscopy (Hadron 91), College Park, August 1991 (to be published); M. Church *et al.*, in Conference Record of the 1991 IEEE Particle Accelerator Conference, San Francisco (unpublished), p. 108.
- [6] T. A. Armstrong *et al.*, Fermilab Report No. FERMILAB-Pub-91/213-E [Nucl. Phys. B (to be published)].
- [7] Particle Data Group, J. J. Hernández *et al.*, Phys. Lett. B **239**, 1 (1990).